

In-situ Gyroscope Calibration Based on Accelerometer Data

Aleksandr Mikov*, Sergey Reginya[†] and Alex Moschevikin[‡]

Petrozavodsk State University

Email: *sasha.mikoff@gmail.com, [†]sreginya@gmail.com, [‡]alexsmou@lab127.karelia.ru

Abstract—The paper presents a novel calibration method for gyroscopes and accelerometers. Contrary to existing methods the proposed one does not require a rotating table or other special equipment. To perform the calibration a user needs to make a series of sequential rotations of inertial measurement unit (IMU) separated by standstills. To find the sensor errors the cost function is defined in terms of orientation differences between accelerometer and gyroscope reported orientations. Then this function is minimized with respect to calibration parameters, that include scale factors, axis non-orthogonalities, biases and misalignment between gyroscope and accelerometer triads.

The proposed method has been verified through Monte-Carlo simulations using synthesized IMU data. Besides the method was tested on real data from MPU-9250 sensors. In both cases, the method was proved to properly find calibration parameters. The simulations revealed that the differences between true and estimated sensor error parameters were less than 0.1% of their true value. The experiments using real and simulated data showed the significant elimination of orientation error after calibration. Moreover, the contribution of gyroscope scale and non-orthogonality errors to the total orientation error was estimated.

The method implementation in Python together with the inertial data simulator and real sensor data are provided publicly *.

Index Terms—gyroscope calibration, inertial sensors.

I. INTRODUCTION

The usage of inertial sensors for positioning and navigation is a well studied field. Usually it is implicitly assumed that the sensors are highly accurate. The desired sensor accuracy can be achieved both by complex manufacturing technologies, and by precise calibration. Optic fiber gyroscope is such a case. MEMS inertial sensors manufacturing process, on the contrary, is relatively simple. This simplicity leads to significant price decrease, and as a consequence, to sensor widespread use on the one hand. On the other hand, MEMS measurement noise, scale factor and bias do not allow their use in areas that require increased accuracy level.

One way to increase sensors' accuracy is to perform the calibration. It is convenient to use turntables [1] and special equipment [2] for this task. During this procedure the IMU is rotated to a number of orientations while the rotation speed and the orientation is precisely controlled and then compared with raw IMU output. However, this approach is inefficient in terms of required time and subsequent expenses [3].

For accelerometer calibration, the alternative approaches have been proposed. Most of them utilize the information about known gravity force vector during standstill periods. As noted in [4], this approach typically leads to a biased estimate of the calibration parameters. To overcome this, the researchers employed the maximum likelihood estimation framework and minimized the cost function both to the sensor calibration parameters and to orientations [5], [6]. Later, [7], this approach was applied to IMU arrays, allowing to estimate not only accelerometer calibration parameters, but also the misalignments between them.

However, to the author's knowledge, there is no such fast, reliable and special equipment free calibration for gyroscopes. To fill this gap we extend the idea of accelerometer [7] calibration using icosahedron to the gyroscope case.

The purpose of this study is to develop a method that allows a simple and complete IMU calibration. The proposed method allows to perform the calibration without special equipment. The user have to make 10-20 arbitrary rotations of the IMU and provide standstill periods. Orientations of the IMU in standstill periods should be different.

The novelty of the proposed approach lies in its specially constructed cost function which allows to evaluate gyroscope errors in addition to the accelerometer's ones. For the accelerometer, the calibration parameters are determined by minimizing the cost function that represents the sum of differences between the measured accelerometer output and the expected one. For gyroscope, the calibration parameters are determined by minimizing the sum of orientation differences between the accelerometer and gyroscope estimated orientations.

The development and verification of the algorithm was performed in several steps. At the first step, IMU data simulator was implemented. At the second step, error cost functions were formulated. These cost functions depend on scale factors of the sensors, non-orthogonality of their axes, biases and misalignment between the accelerometer and gyroscope triads. At the third step, the calibration parameters of the sensors were found using a set of numerical algorithms. At the final step, the estimation of calibration parameters using real data was conducted.

The rest of the paper is organized as follows. Section II describes sensor measurement models for accelerometer and gyroscope. Section III defines the cost functions that can be utilized for finding the sensor calibration parameters using minimization algorithm. In Section IV results from Monte-

*Reproducible research: all files and software for data processing used in experiments and simulations are available under an open-source license at <https://github.com/mikoff/imu-calib>.

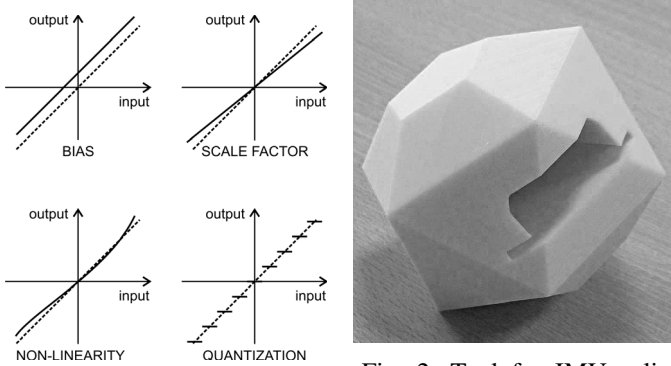


Fig. 1: Sensor error types.

Fig. 2: Tool for IMU calibration.

Carlo simulations and in-house IMU calibrations are presented. The conclusions are given in Section V.

II. SENSOR ERROR MODEL

The sensor error models that show how the main error sources affect accelerometer and gyroscope outputs have the following form:

$$\tilde{\mathbf{f}} = \mathbf{b}_a + (\mathbf{I}_3 + \mathbf{M}_a)\mathbf{f} + \mathbf{w}_a, \quad (1)$$

$$\tilde{\boldsymbol{\omega}} = \mathbf{b}_g + (\mathbf{I}_3 + \mathbf{M}_g)\boldsymbol{\omega} + \mathbf{w}_g, \quad (2)$$

where \mathbf{I}_3 is the 3×3 identity matrix, $\tilde{\mathbf{f}}$ and $\tilde{\boldsymbol{\omega}}$ are the IMU-output specific force and angular rate vectors, \mathbf{f} and $\boldsymbol{\omega}$ are the true counterparts, \mathbf{b}_a and \mathbf{b}_g are the sensor biases, which are the constant errors exhibited by accelerometers and gyroscopes, \mathbf{w}_a and \mathbf{w}_g are the random noises of accelerometers and gyroscopes caused from a number of unmodeled sources. \mathbf{M}_a and \mathbf{M}_g are the matrices, combining the scale factors and cross-coupling errors of accelerometer and gyroscope axes respectively:

$$\mathbf{M}_a = \begin{pmatrix} s_{a,x} & m_{a,xy} & m_{a,xz} \\ 0 & s_{a,y} & m_{a,yz} \\ 0 & 0 & s_{a,z} \end{pmatrix}, \quad (3)$$

$$\mathbf{M}_g = \begin{pmatrix} s_{g,x} & m_{g,xy} & m_{g,xz} \\ 0 & s_{g,y} & m_{g,yz} \\ 0 & 0 & s_{g,z} \end{pmatrix}, \quad (4)$$

where s is the scale factor errors and $m_{\{a,g\},\alpha\beta}$ is the cross-coupling errors, or the non-orthogonality of the sensitive axes, denoting the coefficient of β -axis quantity sensed by the α -axis of the gyroscope or accelerometer sensor.

Due to imperfections in IMU assembling and production the axes triads of accelerometers and gyroscopes are not perfectly aligned. To account for this effect the misalignment rotation matrix \mathbf{R} is added into the model. This matrix describes the orientation between the accelerometer and gyroscope coordinate systems. As noted in [8], when the misalignment is small, the attitude error can be expressed as a vector $\boldsymbol{\epsilon}$ resolved about a chosen set of axes. Then, the rotation matrix \mathbf{R} can be expressed as:

$$\mathbf{R} = \mathbf{I}_3 + [\boldsymbol{\epsilon}]_{\times}, \quad (5)$$

where $[\boldsymbol{\epsilon}]_{\times}$ denotes the skew-symmetric matrix. Having the misalignment error \mathbf{R} introduced, the gyroscope measurements can be transformed to the accelerometer coordinate frame as:

$$\boldsymbol{\omega}^a = \mathbf{R}^{-1}\boldsymbol{\omega}^g. \quad (6)$$

Having the estimates of the biases, scale factors, cross-coupling errors and misalignment between accelerometer and gyroscope, the corrections can be applied:

$$\hat{\mathbf{f}} = (\mathbf{I}_3 + \hat{\mathbf{M}}_a)^{-1}(\tilde{\mathbf{f}} - \hat{\mathbf{b}}_a) \approx (\mathbf{I}_3 + \hat{\mathbf{M}}_a)^{-1}\tilde{\mathbf{f}} - \hat{\mathbf{b}}_a, \quad (7)$$

$$\hat{\boldsymbol{\omega}}^a = (\mathbf{I}_3 + \hat{\mathbf{M}}_g)^{-1}(\hat{\mathbf{R}}^{-1}\tilde{\boldsymbol{\omega}} - \hat{\mathbf{b}}_g) \approx (\mathbf{I}_3 + \hat{\mathbf{M}}_g)^{-1}\hat{\mathbf{R}}^{-1}\tilde{\boldsymbol{\omega}} - \hat{\mathbf{b}}_g \quad (8)$$

The approximated versions of (7) and (8) are obtained by neglecting products of IMU errors, assuming that they are small.

The visualization of the effect of sensor errors on its output is shown in Fig. 1. In the following research the quantization errors are assumed to be small. The performed experiments with the MPU-9250 IMUs (used in this research) on specialized rotation tables revealed that nonlinearities of their input/output curves is negligible proving that the proposed model equations (1) and (2) are valid.

III. CALIBRATION METHOD

The developed accelerometer and gyroscope calibration method does not require any special equipment. It realizes a blind system identification [7] using the prior knowledge about the magnitude of the gravity force vector.

To estimate the calibration parameters contained in $\hat{\mathbf{R}}$, $\hat{\mathbf{M}}_s \in a,g$, $\hat{\mathbf{b}}_s \in a,g$ IMU have to be rotated to a number of different orientations. The process does not imply the prior knowledge of true device orientations thus any applicable tool can be used for this purpose. In the following research, the plastic icosahedron with 22 sides was used (see Fig. 2).

The calibration procedure consists of the following steps.

- 1) Find calibration parameters $\hat{\mathbf{M}}_a$, $\hat{\mathbf{b}}_a$ of the accelerometer.
- 2) Apply calibration parameters to accelerometer output $\tilde{\mathbf{f}}$ and find $\hat{\mathbf{f}}$ according to the equation (7).
- 3) Find gyroscope sensor errors $\hat{\mathbf{R}}$, $\hat{\mathbf{M}}_g$, $\hat{\mathbf{b}}_g$ using the cost function introduced in Sec. III-B.

The cost functions used in optimization routines are defined in the next subsections. The minimization of the following function was done numerically using Trust Region Reflective algorithm [9]. According to our experiments, alternative least squares methods can also be applicable, but they are less stable in terms of finding global minimum.

A. Accelerometer calibration

Let $\{\mathbf{f}_i\}_{i=1}^N$ be a set of averaged accelerometer measurements taken at N different static orientations. Let Θ_a to be nine accelerometer calibration parameters:

$$\Theta_a = [s_{a,x}, s_{a,y}, s_{a,z}, m_{a,yz}, m_{a,xy}, m_{a,xz}, b_{a,x}, b_{a,y}, b_{a,z}] \quad (9)$$

Thus, the squared error between the calibrated accelerometer output \hat{f} and the expected input force $\hat{u}(\phi, \theta)$ can serve as a cost function to calibrate the accelerometer. It is defined as:

$$L(\Theta_a) = \sum_{i=1}^N (f_i - \hat{u}_i(\phi_i, \theta_i))^2, \quad (10)$$

where the expected input force \hat{u} at orientation i depends on pitch and roll angles ϕ_i and θ_i respectively. These pitch and roll angles are calculated from \hat{f} as:

$$\phi_i = \arctan 2 \left(\hat{f}_{a,y}, \hat{f}_{a,z} \right), \quad (11)$$

$$\theta_i = \arctan 2 \left(-\hat{f}_{a,x}, \sqrt{\hat{f}_{a,y}^2 + \hat{f}_{a,z}^2} \right), \quad (12)$$

from which the \hat{u}_i can be calculated as:

$$\hat{u}_i(\phi_i, \theta_i) = [-\sin(\theta_i), \cos(\theta_i) \sin(\phi_i), \cos(\theta_i) \cos(\phi_i)]^T. \quad (13)$$

B. Gyroscope calibration

Let $\{\omega_j\}$, $j = 1 \dots N - 1$, be a set of $N - 1$ series of gyroscope measurements taken while rotating between N static orientations, as described in Sec. III-A (calibration have to be started and ended in standstill conditions).

The characteristic time of rotation j between two orientations is relatively short and takes no more than 1-5 seconds. It means that the gyroscope measurements could be integrated to provide the accurate orientation increment relative to previous static orientation. Therefore, the orientation $R_{g,j}$, computed using gyroscope measurements, at the end of rotation j can be calculated as:

$$R_{g,j} = R_g\{\omega_j\}R_{a,jstart}, \quad (14)$$

where $R_{a,jstart}$ is the static orientation estimate calculated from calibrated accelerometer measurements right before rotation j , $R_g\{\omega_j\}$ is the rotation increment, obtained through integration of calibrated gyroscope measurements ω^a from $\{\omega_j\}$ set. Alternatively, $R_{g,j}$ should be equal to $R_{a,jend}$, meaning that after rotation was completed, the end orientation should be equal to static orientation estimate calculated from calibrated accelerometer measurements.

However, only roll and pitch angles are observable from accelerometer measurements. Thus, the difference between roll and pitch angles should be considered in cost function. Let $R_k^{\phi, \theta} = [R^{\phi}, R^{\theta}]^T$ to be a vector of this angles, extracted from corresponding rotation matrix R_k (alternatively, any other orientation representation can be used).

Let Θ_g to be twelve gyroscope calibration parameters:

$$\Theta_g = [s_{g,x}, s_{g,y}, s_{g,z}, m_{g,yz}, m_{g,xy}, m_{g,xz}, b_{g,x}, b_{g,y}, b_{g,z}, \epsilon_x, \epsilon_y, \epsilon_z] \quad (15)$$

TABLE I: DIFFERENCE BETWEEN TRUE AND ESTIMATED SENSOR ERROR PARAMETERS FOR 200 MONTE-CARLO SIMULATIONS. THE AVERAGE ERROR IN PARAMETERS ESTIMATION TOGETHER WITH ITS STANDARD DEVIATION IS SHOWN.

Param.	Parameter estimation error, $\Theta_{true} - \Theta_{est}$					
	Accelerometer			Gyroscope		
	Average	Standard deviation	Units	Average	Standard deviation	Units
s_x	-0.0	0.0002		0.0003	0.0005	
s_y	-0.0001	0.0004		0.0003	0.0006	
s_z	0.0	0.0004		0.0004	0.0021	
m_{yz}	-0.0057	0.0286	°	-0.0057	0.1891	°
m_{xy}	0.0	0.0286	°	-0.0115	0.1318	°
m_{xz}	-0.0	0.0344	°	0.0115	0.0688	°
b_x	-0.0003	0.0019	m/s^2	-0.0172	0.0344	°/s
b_y	-0.0	0.0031	m/s^2	0.0	0.0286	°/s
b_z	-0.0002	0.0031	m/s^2	0.0	0.0229	°/s
ϵ_x	—	—		-0.0	0.0974	°
ϵ_y	—	—		-0.0	0.0286	°
ϵ_z	—	—		-0.0057	0.0401	°

Now the cost function for gyroscope calibration can be defined as:

$$L(\Theta_g) = \sum_{j=1}^M \left(\left(R_{a,jend} R_{g,j}^T \right)^{\phi, \theta} \right)^2 = \sum_{j=1}^M \left(\left(R_{a,jend} (R_g\{\omega_j\} R_{a,jstart})^T \right)^{\phi, \theta} \right)^2, \quad (16)$$

where the product $R_{a,jend} R_{g,j}^T$ describes the rotation of the gyroscope relative to the accelerometer.

IV. EXPERIMENTS AND RESULTS

A. Simulations

To test the performance of the proposed calibration method the Monte-Carlo simulations were performed. The ideal accelerometer and gyroscope measurements were generated while the IMU was rotated sequentially from one to another random orientation and kept static after each rotation. The total number of orientations was equal to 24. The rotation time between two static orientations was set to one second, the time, for which IMU was held static at each orientation was also equal to one second.

Then these ideal IMU measurements were corrupted according to equations (1), (2) and (6). The accelerometer and gyroscope scale factor errors were randomly chosen in range $(-0.1, 0.1)$, the cross-coupling of axes in range $(-0.06, 0.06)$, which is equal to $\pm 5.7^\circ$. The accelerometer bias was chosen to be in range of $(-1, 1) m/s^2$, the gyroscope bias – in range of $(-6, 6)^\circ/s$, the misalignment between accelerometer and gyroscope triads – in range of $(-6, 6)^\circ$. The distribution of choosed values was uniform. White noise parameters w_a and w_g were set to $\mathcal{N}(0.0, 0.04) m/s^2$ and $\mathcal{N}(0.0, 0.001) rad/s$ respectively. These standard deviations reflect the noise level of commercial off-the-shelf IMUs [10]. After that, the calibration was performed using the method described in Sec. III.

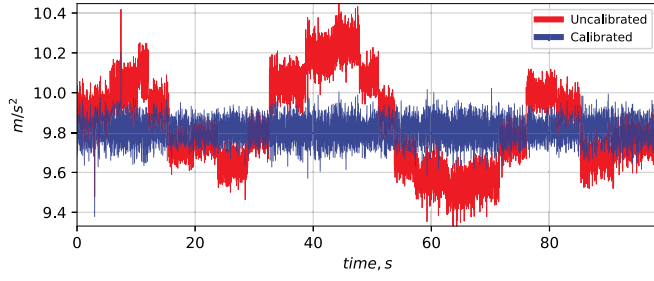


Fig. 3: IMU#1 accelerometer measurement magnitudes before and after calibration are shown in red and blue colors respectively.

The results of 200 Monte-Carlo simulations are shown in Table I. It is seen that the mean difference between true and estimated sensor error parameters is close to zero and relatively small compared to the absolute value of sensor errors. These results indicate that the method is unbiased both for accelerometer and gyroscope calibration procedures.

B. Experiments

The proposed calibration method was tested using MIMU2.5 multisensor inertial module [11], [12]. It includes a microcontroller obtaining acceleration and rotation rate samples from five InvenSense MPU-9250 chips.

MIMU2.5 module was placed inside the plastic calibration tool, shown on Fig. 2. The tool was rotated to different orientations and data obtained from all five MPU-9250 sensors were synchronized and recorded separately. Then the data were marked automatically to be static or not based on measurements magnitude and fed to the calibration method.

Since the estimated calibration parameters do not give information whether the calibration was successful, it is important to verify the results. In this research, it is done through assessment of the sum of gyroscope calibration residuals. If it is less than 3.0° then the found calibration parameters are assumed to be correct, since it is very unlikely to have such a small orientation difference if the calibration parameters are incorrect.

The estimated calibration parameters for IMUs are shown in Table II. It became evident that the IMU factory calibration quality is high enough and lie within the region, allowed by the sensor's datasheet. The scale factor error is less than 1% both for accelerometers and gyroscopes. The non-orthogonality of axes and misalignment between triads is less than 1° for all tested sensors.

The magnitudes of uncalibrated and calibrated accelerometer output during standstill periods for IMU#1 are shown on Fig. 3.

Since the gyroscope bias calibration is trivial, it is interesting to see how the gyroscope scale, cross-coupling and misalignment errors affect the orientation solution when the bias is known. The total rotation time for each experiment was equal to 58 seconds. During this time the orientation error

TABLE II: IMUS CALIBRATION RESULTS.

Param.	Accelerometer					Gyroscope				
	#1	#2	#3	#4	#5	#1	#2	#3	#4	#5
$s_x, \%$	0.363	0.471	0.382	0.263	0.251	0.041	0.007	-0.058	0.227	0.226
$s_y, \%$	0.315	0.482	0.355	0.448	0.286	0.457	0.26	0.277	0.599	0.57
$s_z, \%$	0.647	0.932	0.78	0.721	0.804	0.826	-0.179	0.242	0.308	0.853
$m_{xz}, ^\circ$	0.123	-0.284	0.26	-0.009	0.056	-0.034	-0.639	0.15	-0.105	0.08
$m_{xy}, ^\circ$	0.02	-0.01	-0.012	-0.028	0.0	-0.12	0.21	-0.072	0.025	0.178
$m_{yz}, ^\circ$	0.317	0.145	0.282	-0.104	0.191	0.806	0.262	0.876	0.072	0.497
$b_x, ^\circ$	0.103	0.09	0.096	0.065	0.07	1.146	-0.573	0.573	-1.261	-1.031
$b_y, ^\circ$	0.097	0.07	0.008	0.092	0.036	-0.401	1.089	-0.344	1.031	0.401
$b_z, ^\circ$	0.344	0.338	-0.045	-0.009	0.182	1.261	0.286	0.286	4.813	1.432
$\epsilon_x, ^\circ$	-	-	-	-	-	0.03	-0.565	0.142	-0.102	0.077
$\epsilon_y, ^\circ$	-	-	-	-	-	-0.364	0.013	-0.482	-0.129	-0.223
$\epsilon_z, ^\circ$	-	-	-	-	-	-0.074	0.069	-0.079	0.015	0.075

*. b_x , b_y and b_z are in m/s^2 and in $^\circ/s$ for accelerometer and gyroscope respectively.

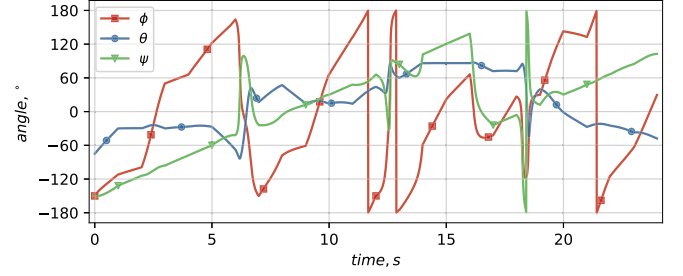


Fig. 4: Rotation profile to estimate the orientation difference between true orientations and the restored one.

induced by s_g and m_g with respect to accelerometer orientation for all IMUs lied in ranges $[3.1 - 3.9]^\circ$ and $[3.3 - 4.9]^\circ$ for ϕ and θ angles respectively. As a result of s_g and m_g estimation, the errors were reduced significantly and lied in ranges $[0.1 - 0.5]^\circ$ to $[0.1 - 0.6]^\circ$ for ϕ and θ angles.

To visualize how these errors affect the estimated orientation the sensor parameters for IMU#1 was injected into the simulation model. The IMU was rotated smoothly between 24 randomly generated orientations without standstill periods. Then three sets of orientation differences between true orientations and:

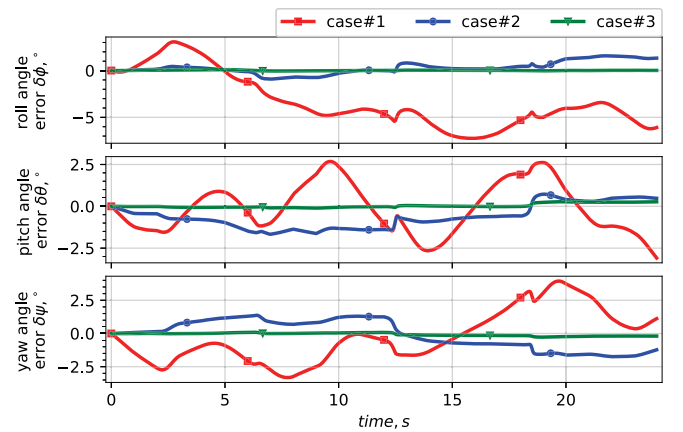


Fig. 5: The orientation errors when: case#1 – no corrections of gyroscope raw data, case#2 – only gyroscope bias was corrected, case#3 – gyroscope scale error, cross-coupling and bias were corrected.

- 1) orientations, obtained by integration of uncalibrated gyroscope outputs,
- 2) orientations, obtained by integration of partially calibrated gyroscope outputs (only bias),
- 3) orientations, obtained by integration of fully calibrated gyroscope using the proposed method

were calculated. The rotation profile (orientation changes, for which IMU output was generated) is shown on Fig 4.

The orientation differences for roll, pitch and yaw angles for these cases are shown on Fig. 5. It is clearly seen that even when the gyroscope bias was corrected the scale and cross-coupling errors of the gyroscope induce significant orientation error even on short time intervals. For example, in this particular simulation the orientation error caused by these errors was up to 3° for each euler angle during rotation. After calibration the euler angles errors did not exceed 0.1° , verifying the significance of full gyroscope calibration.

V. CONCLUSION

The accelerometer and gyroscope calibration method that does not require reference information about rotation velocity or orientation was proposed. The calibration procedure utilizes only the accelerometer and gyroscope outputs during a series of rotations between different orientations. These rotations have to be separated by short standstill periods. No other constraints are imposed.

Parameters of an accelerometer-gyroscope chip/module that can be calibrated: a) biases, b) scale factors, c) axis non-orthogonalities, and d) misalignment between gyroscope and accelerometer triads.

Gyroscope parameters are determined by comparison of the orientation angles obtained from acceleration data in static conditions and accumulated orientation change calculated from the gyroscope output during rotation phase.

The calibration method has been shown to give consistent unbiased estimates of true sensor errors parameters within 0.1% of their absolute true value. The results were verified using simulated and real data. The simulations approved the significance of full gyroscope calibration in comparison with bias consideration only.

The simplicity and robustness of the method make it a good tool for engineers and researches that are interested in improvement of their low-cost three-axial inertial sensors. The open-sourced solution will help to distribute the results and reproduce the presented calibration procedure in-house.

REFERENCES

- [1] Rui Zhang, Fabian Hoffinger, and Leonhard M Reind. Calibration of an imu using 3-d rotation platform. *IEEE sensors Journal*, 14(6):1778–1787, 2014.
- [2] Olli Särkkä, Tuukka Nieminen, Saku Suuriniemi, and Lauri Kettunen. A multi-position calibration method for consumer-grade accelerometers, gyroscopes, and magnetometers to field conditions. *IEEE Sensors Journal*, 17(11):3470–3481, 2017.
- [3] Sara Stančin and Sašo Tomažič. Time-and computation-efficient calibration of mems 3d accelerometers and gyroscopes. *Sensors*, 14(8):14885–14915, 2014.
- [4] Ghazaleh Panahandeh, Isaac Skog, and Magnus Jansson. Calibration of the accelerometer triad of an inertial measurement unit, maximum likelihood estimation and cramer-rao bound. In *2010 International Conference on Indoor Positioning and Indoor Navigation*, pages 1–6. IEEE, 2010.
- [5] Fredrik Olsson, Manon Kok, Kjartan Halvorsen, and Thomas B Schön. Accelerometer calibration using sensor fusion with a gyroscope. In *2016 IEEE Statistical Signal Processing Workshop (SSP)*, pages 1–5. IEEE, 2016.
- [6] Pablo Bernal-Polo and H Martínez-Barberá. Triaxial sensor calibration: A prototype for accelerometer and gyroscope calibration. In *Iberian Robotics conference*, pages 79–90. Springer, 2017.
- [7] John-Olof Nilsson, Isaac Skog, and Peter Händel. Aligning the forces—eliminating the misalignments in imu arrays. *IEEE Transactions on Instrumentation and Measurement*, 63(10):2498–2500, 2014.
- [8] Paul D Groves. Principles of gnss, inertial, and multisensor integrated navigation systems, [book review]. *IEEE Aerospace and Electronic Systems Magazine*, 30(2):26–27, 2015.
- [9] Mary Ann Branch, Thomas F Coleman, and Yuying Li. A subspace, interior, and conjugate gradient method for large-scale bound-constrained minimization problems. *SIAM Journal on Scientific Computing*, 21(1):1–23, 1999.
- [10] Invensense. Mpu 9250 datasheet. USA: InvenSense, 2016.
- [11] A. Moschevikin, A. Sikora, P. Lunkov, A. Fedorov, and E. Maslennikov. Hardware and software architecture of multi mems sensor inertial module. In *24th Saint Petersburg International Conference on Integrated Navigation Systems (ICINS)*, pages 366–369, 2017.
- [12] Manuel Schwaab, Sergey Reginya, Axel Sikora, and Evgenii Abramov. Measurement analysis of multiple mems sensor array. In *2017 24th Saint Petersburg International Conference on Integrated Navigation Systems (ICINS)*, pages 1–4. IEEE, 2017.